JOURNAL OF GEOPHYSICAL RESEARCH, VOL. 104, NO. A11, PAGES 24,613–24,624, NOVEMBER 1, 1999

Coherent EISCAT Svalbard Radar spectra from the dayside cusp/cleft and their implications for transient field-aligned currents

K. J. F. Sedgemore-Schulthess,[1] M. Lockwood,[2] T. S. Trondsen,[3]
B. S. Lanchester,[1] M. H. Rees,[1] D. A. Lorentzen,[4] and J. Moen[4]

Abstract. Naturally enhanced incoherent scatter spectra from the vicinity of the dayside cusp/cleft, interpreted as being due to plasma turbulence driven by short bursts of intense field-aligned current, are compared with high-resolution narrow-angle auroral images and meridian scanning photometer data. Enhanced spectra have been observed on many occasions in association with nightside aurora, but there has been only one report of such spectra seen in the cusp/cleft region. Narrow-angle images show considerable change in the aurora on timescales shorter than the 10-s radar integration period, which could explain spectra observed with both ion lines simultaneously enhanced. Enhanced radar spectra are generally seen inside or beside regions of 630-nm auroral emission, indicative of sharp *F* region conductivity gradients, but there appears also to be a correlation with dynamic, small-scale auroral forms of order 100 m and less in width.

1. Introduction

Incoherent scatter radars are designed to detect extremely weak echoes from thermally driven ion-acoustic waves in the ionosphere. Departures from the two-shouldered ion spectra characteristic of incoherent backscatter from thermal plasma have been studied for a number of years, mostly in relation to non-Maxwellian plasma distributions. Enhancements in one or the other of the spectral peaks have also aroused interest. Spectral enhancements are associated with hard targets such as satellites when seen over restricted height ranges and as such are generally discarded at the data reduction stage. When observed over extended height ranges, such enhancements have been interpreted as due to destabilization of ion-acoustic waves [*Rosenbluth and Rostoker,* 1962].

One theory proposed to account for destabilization of ion-acoustic waves is based on intense field-aligned currents [e.g., *Collis et al.,* 1991; *Rietveld et al.,* 1991]. The densities required ($\sim$1 mA m^{-2}) are not unreasonable if the currents are discharged quickly and/or the width of the layers is small [*Collis et al.,* 1991; *Cabrit et al.,* 1996]. A firm theoretical basis for the study of topside current instabilities has been laid by *Kindel and Kennel* [1971]. *St.-Maurice et al.* [1996] discuss the inferred field-aligned currents in terms of intense parallel electric fields of up to a few hundred microvolts per meter in magnitude together with horizontal scales of a few hundred meters or less. *Forme* [1993] has suggested that ion-acoustic fluctuations may be due to parametric decay of Langmuir waves, and *Wahlund et al.* [1992a] propose a theory based on ion-ion two-stream instabilities.

Measurements made by *Foster et al.* [1988] using the Millstone Hill 440-MHz radar at angles of at least 11° away from the local magnetic field direction revealed echoes that could easily have been mistaken for satellite passes had they not had a consistent altitude profile and come from a fixed region of space. It is quite likely that the enhancement in *F* region backscattered power observed by *Hapgood and Lanchester* [1987] during the passage of a narrow auroral arc through the EISCAT (European Incoherent SCATter) beam at Tromsø, and interpreted at the time as being due to an enhanced ionization rate, was in fact due to the presence of unstable ion-acoustic waves associated with the arc. Owing to an error with the receiver configuration, no spectra are available with which to verify this. Also using the EISCAT 933-MHz UHF system, a number of authors have reported on enhanced spectra. *Collis et al.* [1991] state that in the cases they observed, the events coincided with the edges of intense 630-nm auroral arcs at high altitudes. *Rietveld et al.* [1991] present measurements taken mainly from along the magnetic field direction and suggest that field-aligned flows of soft electrons are the cause of parallel electric fields in the ionosphere producing thermal electron drifts that lead to enhanced radar spectra.

Wahlund et al. [1992b] discuss EISCAT observations of topside ion outflows, noting that enhanced radar spectra are often observed during so-called "type 2" plasma outflows

[1]Department of Physics and Astronomy, University of Southampton, Hampshire, England.
[2]Space Science Department, Rutherford Appleton Laboratory, Oxfordshire, England.
[3]Department of Physics and Astronomy, University of Calgary, Alberta, Canada.
[4]Universitetsstudiene på Svalbard, Longyearbyen, Norway.

Paper number 1999JA900276.
0148-0227/99/1999JA900276$09.00

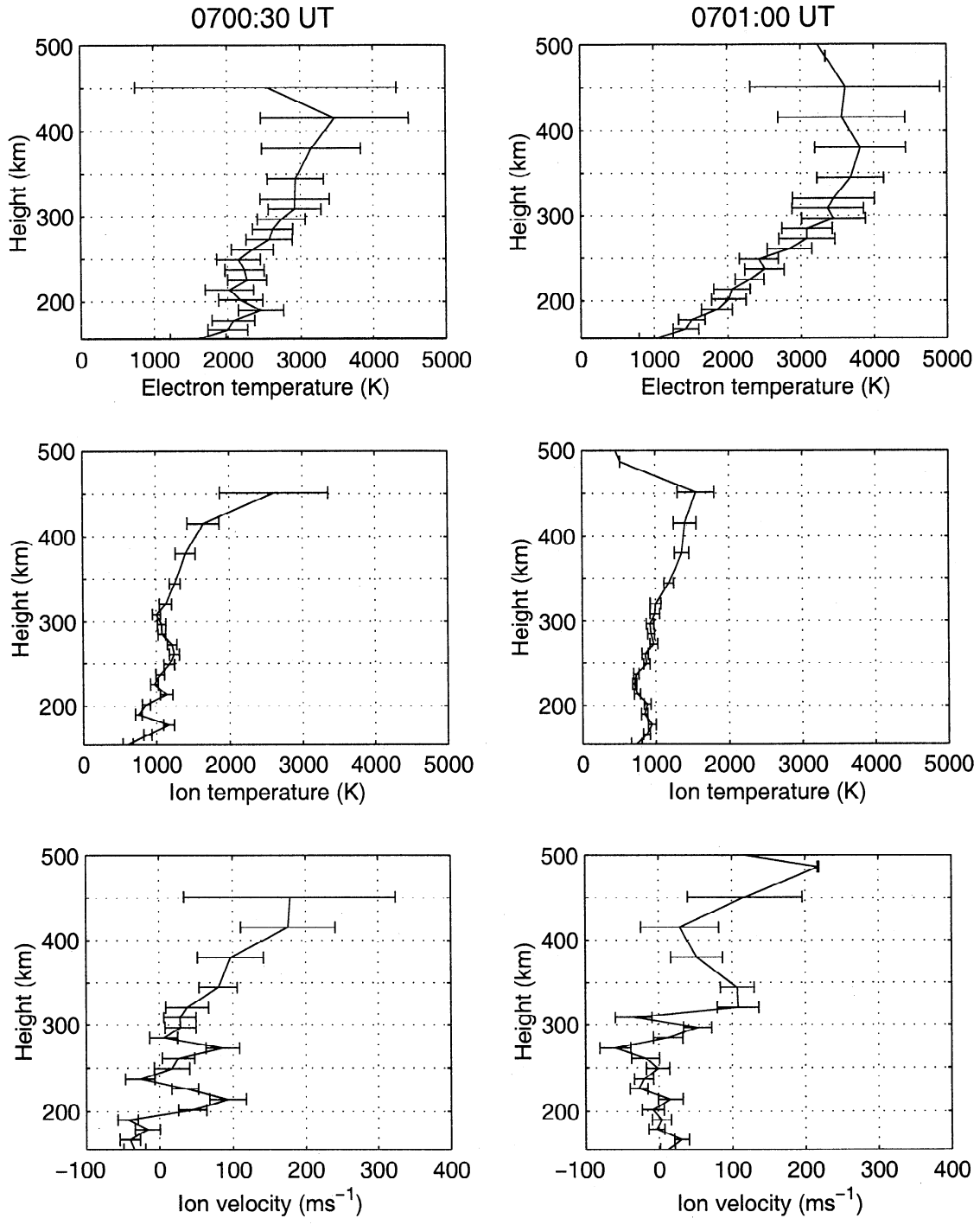

Figure 2. Electron and ion temperatures and line-of-sight ion velocity derived from EISCAT Svalbard Radar data, 0700:30 and 0701:00 UT, January 24, 1998.

topside ion outflow is considerably smaller than the maximum values recorded during this 3-hour period.

Figure 6 displays a sequence of 20 PAI images starting at 0706:30 UT. As with the previous example, there is much change within the period, with coronal forms seen until 0706:35 UT, after which almost all the emission is concentrated in the zenith. There is a common element in Figures 3 and 6 in that strong coronal forms are seen only in the 10-s periods when the upshifted ion-acoustic line is enhanced. We can only loosely associate the in-beam luminosity with enhanced downshifted ion lines. In all the cases that we have found of enhanced downshifted lines, there is in-beam luminosity, but this may be strong, as in Figure 6, or weak, as in Figure 3. Furthermore, there are several intervals of in-beam luminosity in the period that do not result in downshifted enhancements, and in none of the cases does in-beam lumi-

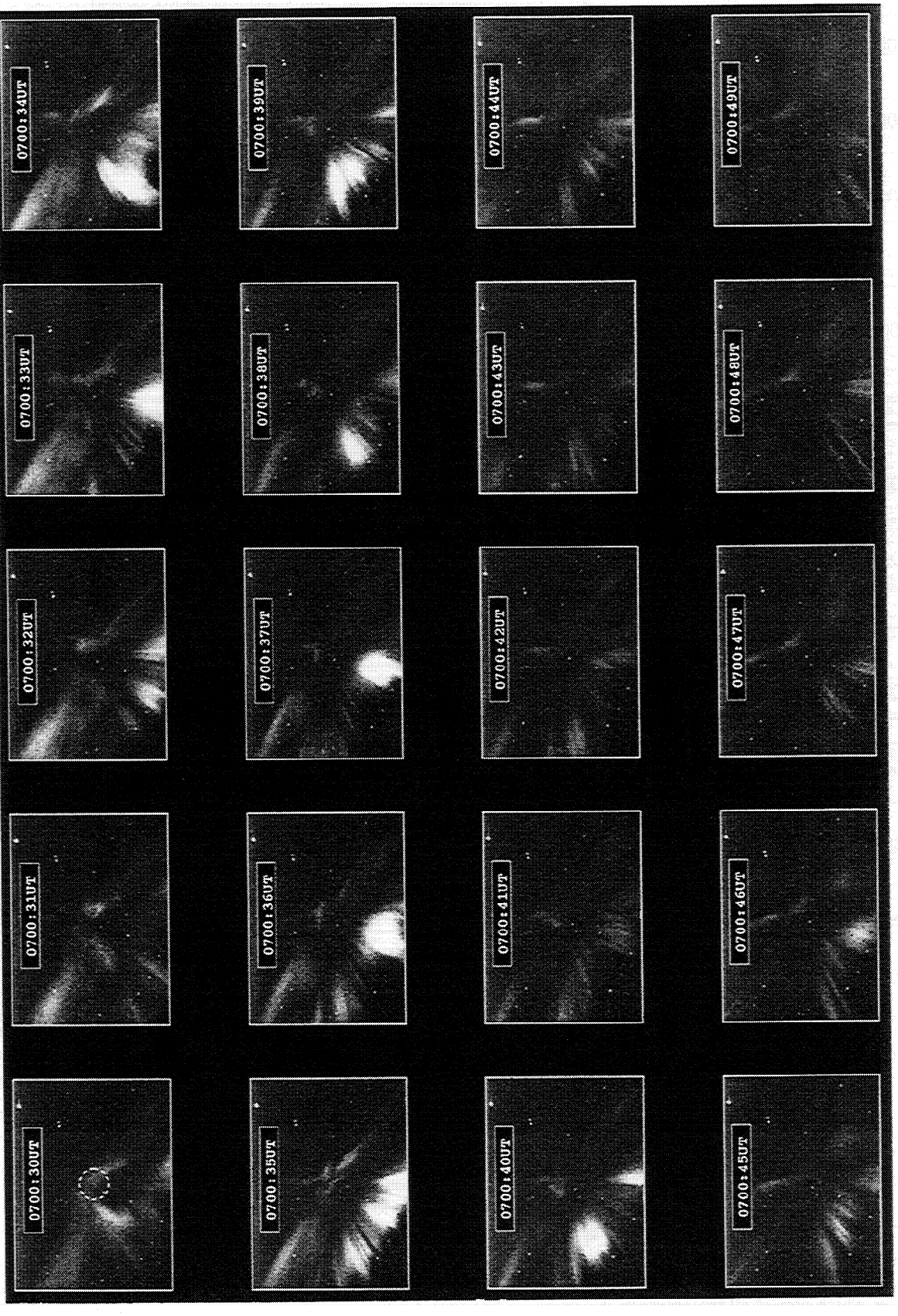

Figure 3. Narrow-angle images from the Portable Auroral Imager in Adventdalen, 0700:30–0700:49 UT, January 24, 1998. In each image, four video frames are averaged in order to improve the signal-to-noise ratio, and an enhanced scale is used to compensate for losses due to the 675-nm cutoff filter. In these images north is at the top and east is to the right, and the sequence goes from left to right, top to bottom. In the top left image the circle represents the position and size of the radar beam.

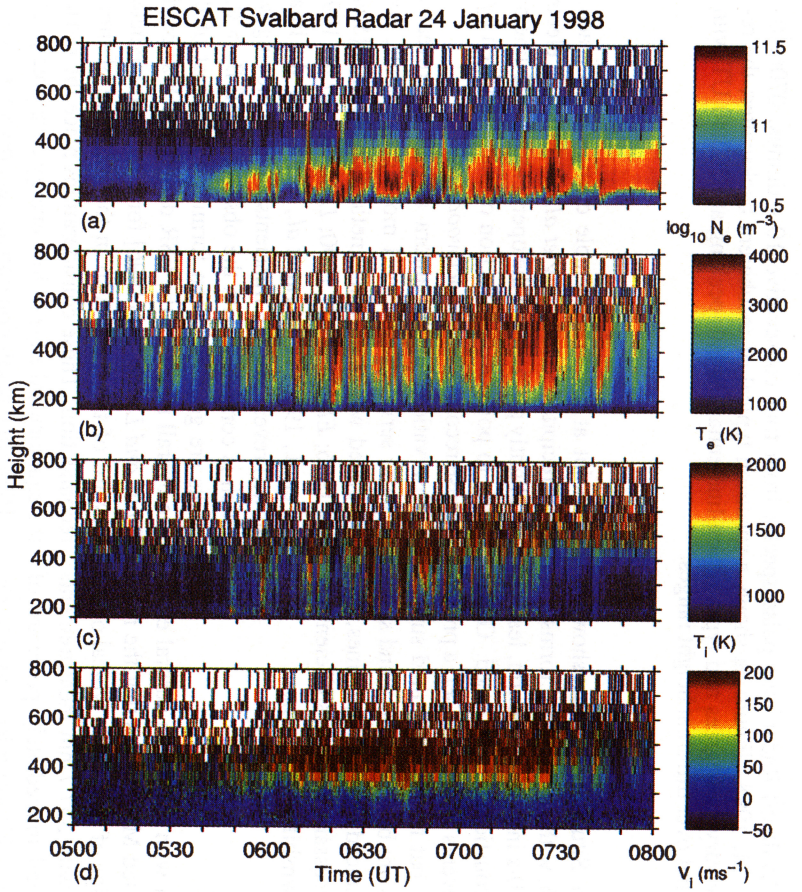

Plate 1. *F* region ionospheric parameters at 10-s resolution derived from EISCAT (European Incoherent SCATter) Svalbard Radar data, 0500–0800 UT, January 24, 1998. From top to bottom, the panels represent (a) electron density, (b) electron temperature, (c) ion temperature and (d) line-of-sight ion velocity.

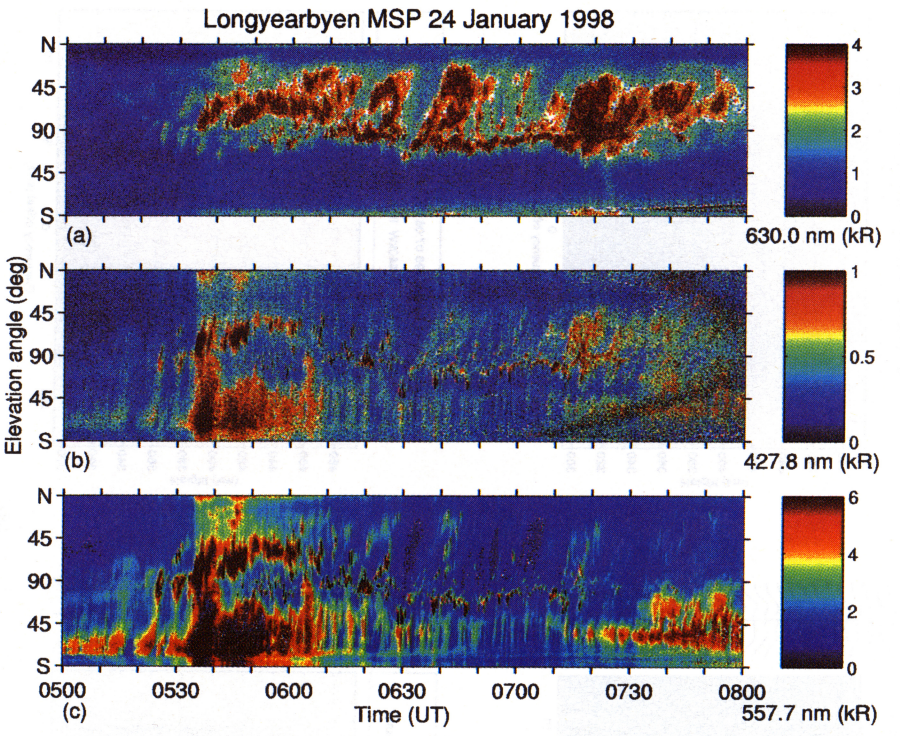

Plate 2. Column emission rates derived from Meridian Scanning Photometer (MSP) data at 16-s resolution, 0500–0800 UT, January 24, 1998. From top to bottom, the panels represent peak minus base measurements for (a) 630.0-nm, (b) 427.8-nm, and (c) 557.7-nm auroral emissions.

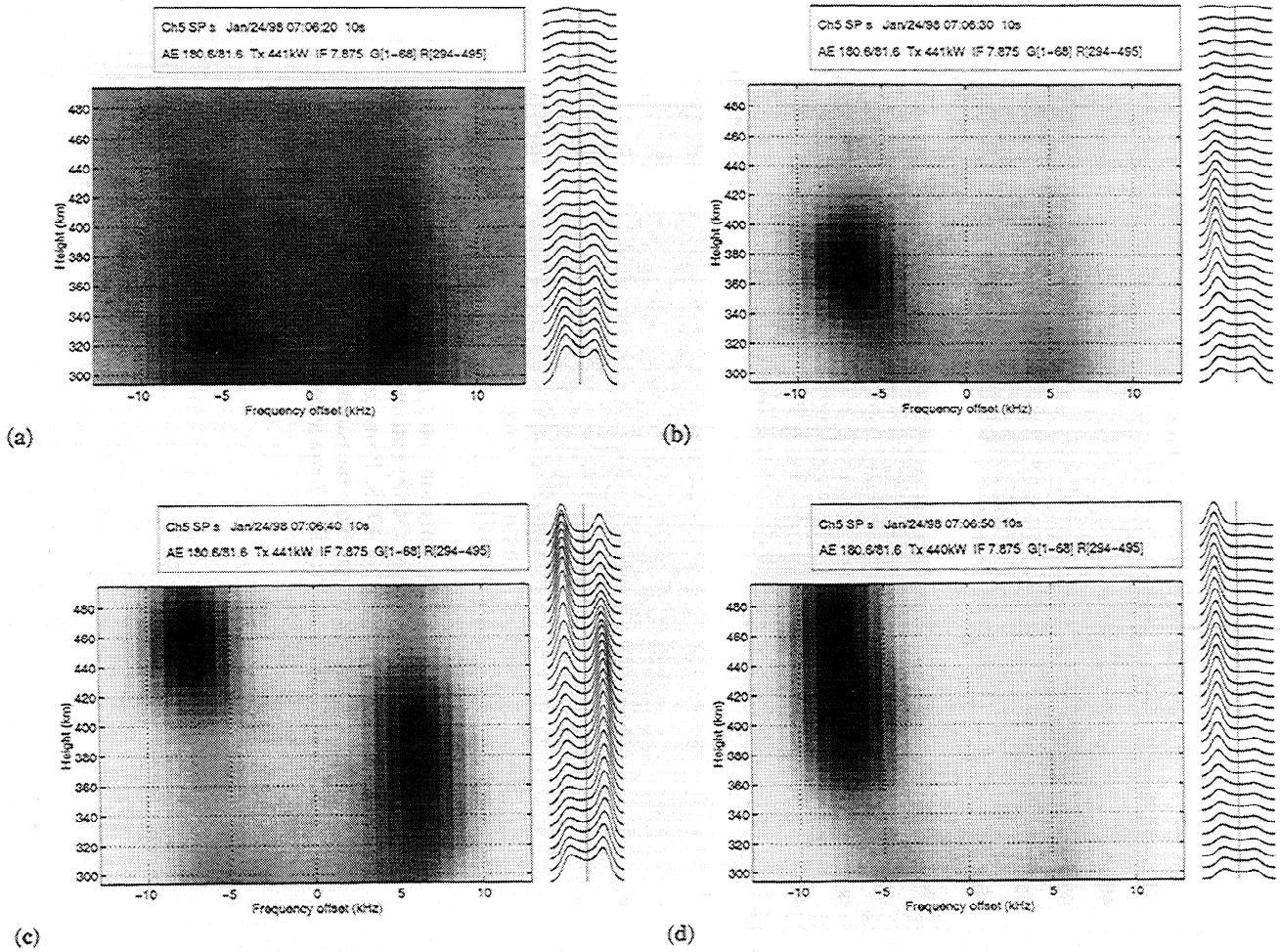

Figure 4. EISCAT Svalbard Radar long-pulse spectra from four consecutive 10-s dumps, 0706:20–0706:50 UT, January 24, 1998. Figure 4a shows a spectrum typical of incoherent backscatter; the remaining figures show varying degrees and types of ion-line enhancement, peaking at 0706:40 UT with both lines enhanced, but over different height ranges.

nosity completely fill the beam. Situations like that shown in the first 10 s of Figures 3 and 6, with both coronal forms and bright patches seen within a 10-s integration period, lead to radar spectra with both ion-acoustic lines enhanced. Given that we have found only five events in this data set, a proper statistical test is not possible, but from this limited survey we suggest that coronal forms are both necessary and sufficient for the formation of enhanced upshifted ion lines, and that in-beam luminosity is necessary, but not sufficient for the formation of enhanced downshifted ion lines.

4. Discussion

A comparison of ESR data with 630.0-nm auroral emissions measured with a colocated MSP shows that the radar is close to the equatorward edge of red aurora typical of the cusp. A similar comparison with 557.7-nm measurements shows that the beam is located immediately poleward of green-line aurora enhanced by substorm injections into the ring current, placing it in a region poleward of both the open-closed field-line boundary and the electron edge, which is the point at which detectable change takes place in electron precipitation [*Gosling et al.,* 1990]. The electron edge lies slightly poleward of the open-closed field-line boundary, owing to poleward convection of plasma driven by magnetopause reconnection [*Lockwood,* 1997].

Observations of the aurora at 630 nm reveal a quasi-periodic series of poleward moving transients, commonly associated with pulsed magnetic reconnection [*Sandholt et al.,* 1986; *Elphic et al.,* 1990; *Lockwood et al,* 1993; *Karlson et al.,* 1996; *Farrugia et al.,* 1998]. All-sky images (not shown) reveal that the transients are also moving westward, which is consistent with the observed IMF $B_y > 0$, and the events are generally seen forming to the east of the radar. The overall nature of the ESR data is much as predicted by *Davis and Lockwood* [1996] for a radar immediately equatorward of the main cusp in the presence of time-varying reconnection. These considerations place the radar close to the equatorward edge of low-energy cusp precipitation.

High time resolution optical data reveal that care must be taken when interpreting radar spectra observed with both ion lines simultaneously enhanced. Given that these data were

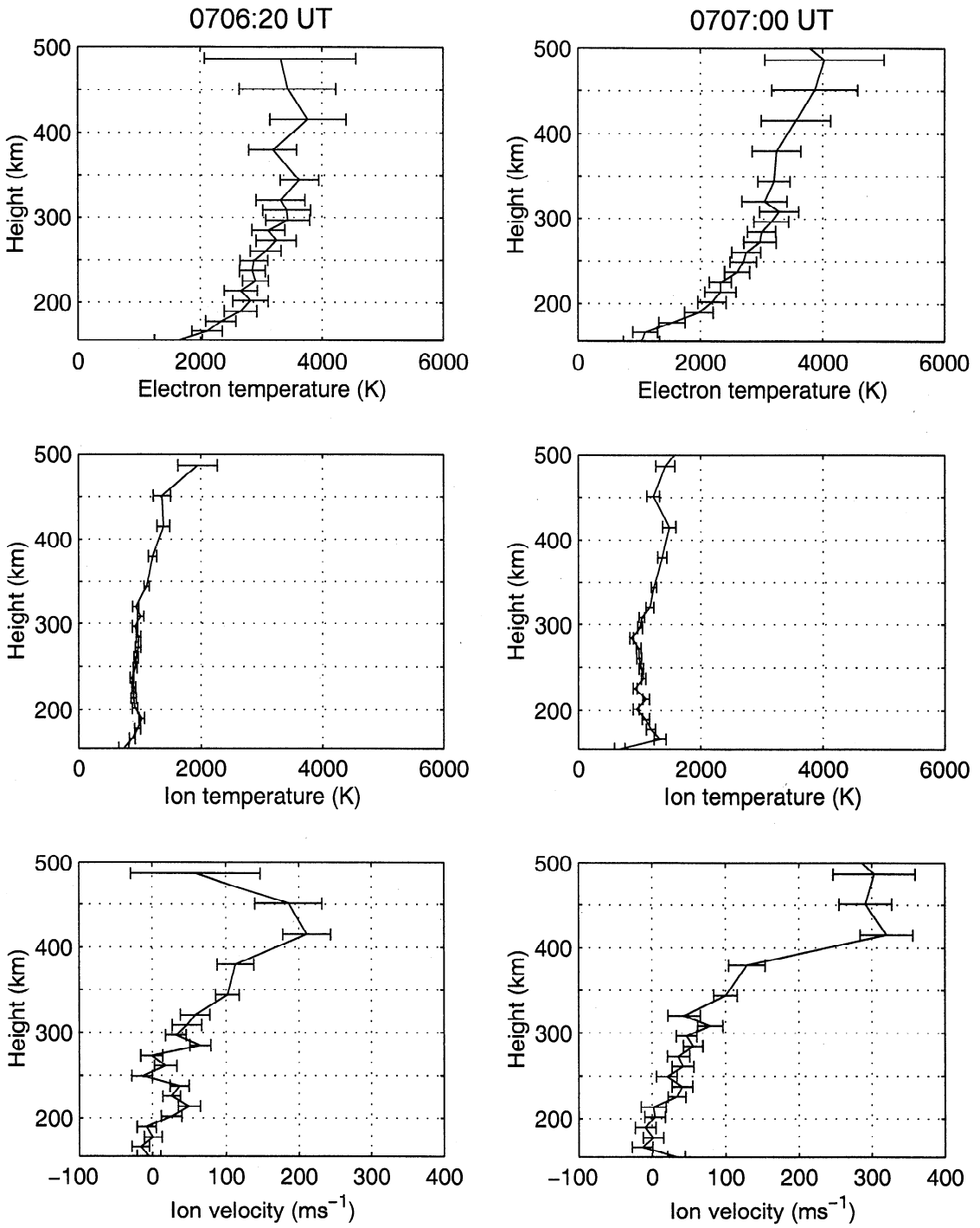

Figure 5. Electron and ion temperatures and line-of-sight ion velocity derived from EISCAT Svalbard Radar data, 0700:20 and 0707:00 UT, January 24, 1998.

recorded with a 10-s integration, no direct information is available on timescales shorter than this. Narrow-angle auroral images, however, show considerable change in the aurora within such a period. We found change within the integration period from bright luminosity in the beam to little or no luminosity, but common to all the events are coronal forms and patches of luminosity in the zenith, indicating that the precipitation is on field lines probed by the radar and those directly adjacent to the beam, respectively.

This questions the idea that two enhanced shoulders ever coexist on one magnetic field line and deals therefore with the objection of *Wahlund et al.* [1992a] to electron ion-acoustic instabilities being the cause of the enhanced radar spectra. Two-stream instabilities do not require the very high current densities needed to explain the spectra in terms of electron ion-acoustic instabilities, but they do require that the ion drift velocity be of the order of its thermal velocity. This is unlikely to be the case except at very high altitudes,

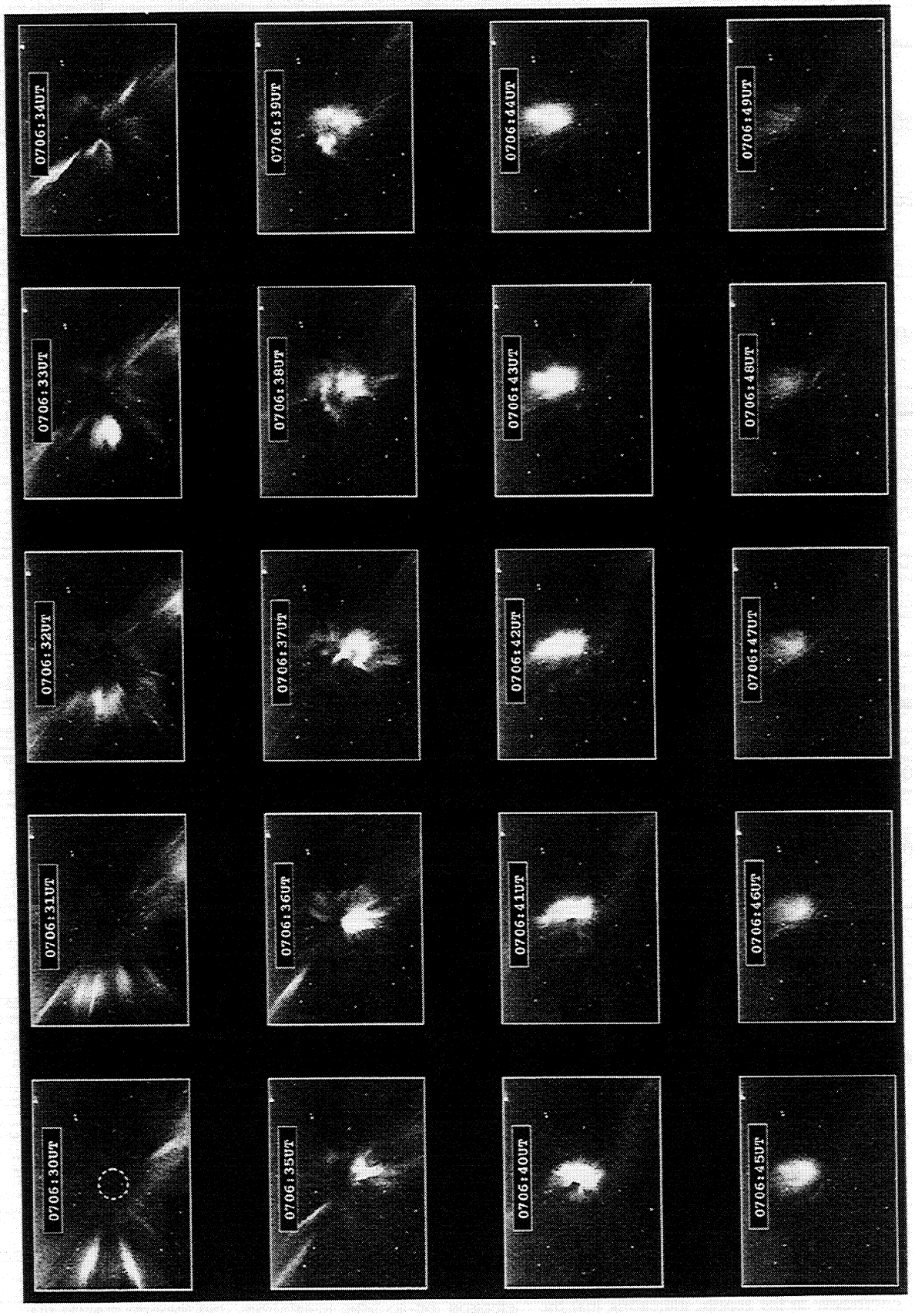

Figure 6. Narrow-angle images from the Portable Auroral Imager in Adventdalen, 0706:30–0706:49 UT, 24 January 1998. In these images north is at the top and east to the right, and the sequence goes from left to right, top to bottom. In the top left hand image there is a circle representing the position and size of the radar beam.

where the ion collision frequency is low, and lower plasma densities require larger ion velocities to carry a given magnitude of flux. The Langmuir wave theory proposed by *Forme* [1993] allows for a significant reduction in the field-aligned current threshold, but some of the implications of the theory have not yet been worked through [e.g., *Cabrit et al.*, 1996]. Despite these criticisms it remains the only serious alternative to the current-driven instability model.

Other relevant questions concern the height distribution of enhanced radar spectra and the degree of aspect sensitivity. A streaming instability can exist at any angle for which the drift speed exceeds the threshold condition, which would explain why *Foster et al.* [1988] could observe spectral enhancements at an aspect angle of 11°, although only in the highest altitude gates. *Rietveld et al.* [1991] show that spectral enhancements at lower altitudes are seen more often when the radar beam is field-aligned. A local field-aligned current will change the orientation of the field line and therefore shift the position of the magnetic zenith. Using auroral images, *Velichko et al.* [1985] traced the converging rays in coronal forms in order to determine the shift in the zenith and found a scatter in radiant points as large as 8°. While the limitations in their approach may lead one to question such a large scatter, a shift of a few degrees is to be expected from observed auroral currents. The direction of the radar beam with respect to the local magnetic field could then become significant, as the radar would be sampling across different field lines, in which case field-perpendicular spatial structure would become apparent along the radar beam. This spatial aliasing could lead to both ion-acoustic lines being enhanced within a single integration period.

In common with previous studies [e.g., *Rietveld et al.*, 1991; *Rietveld et al.*, 1996], our data show that the downshifted ion line is enhanced preferentially at higher altitudes. From our results we suggest that within a single radar integration period the beam can for part of the time be within a region of downward field-aligned current carried by upgoing thermal electrons, and the PAI images suggest that this is when bright auroral luminosity is seen in the radar beam. The upgoing thermal electrons drive nonthermal spectra at higher altitudes, where densities are lower and the velocities, owing to current continuity, are larger. Within the same integration period we may be observing nonthermal spectra at lower altitudes in regions of upward field-aligned current caused by downward flows of thermalized electrons required by current continuity [e.g., *Rietveld et al.*, 1991; *St.-Maurice et al.*, 1996]. Note that only thermal electrons can carry the current magnitudes required to destabilize ion-acoustic waves; we do not attempt to explain any connection between energetic electron precipitation and transient field-aligned currents. The regions adjacent to these filamentary field-aligned currents would most likely be part of the same current system, implying that large electric fields and Pedersen currents exist between them. On the other hand, the relatively low ion temperatures seen before and after the enhanced echoes indicate that the Pedersen current closure is highly localized such that little electric-field-induced ion heating is present around the current structures.

In this study we have assumed explicitly a current-driven instability model and invoked the presence of intense field-aligned currents in order to explain the observed spectra. Modeling work based on Alfvén wave propagation shows that large-magnitude filamentary field-aligned currents can exist in the ionosphere in response to plasma velocity shears associated with magnetic reconnection, and that energetic auroral precipitation can further constrain the width of the current layers (A. Otto, personal communication, 1999). As for observational evidence, *Stasiewicz and Potemra* [1998] and *Stasiewicz et al.* [1998] report on density depletions and small-scale field-aligned currents with magnitudes of up to 300 μA m^{-2} observed with the Freja satellite. Preliminary results from the Astrid 2 satellite show filamentary field-aligned currents with magnitudes of around 250 μA m^{-2}, together with horizontal separations between upgoing and downgoing current layers of less than 10 km (G. Marklund, personal communication, 1999).

5. Summary

We have presented observations of coherently enhanced ion-acoustic spectra seen by the EISCAT Svalbard Radar. Enhanced spectra have been reported previously from the Millstone Hill and mainland EISCAT radars in the vicinity of the nightside auroral zone, but there has been only one report of enhanced spectra in the cusp/cleft region [*Buchert et al.*, 1999]. Our observations are close to the latitude and local time of solar wind precipitation into the dayside cusp/cleft.

Around the time that the enhanced radar spectra were seen, scanning photometer measurements reveal a series of poleward moving auroral transients, possibly indicating an association between transient field-aligned currents, which we believe to be the cause of the nonthermal spectra, and pulsed magnetopause reconnection. East-west motion of the transients is consistent with the observed IMF $B_y > 0$, and erosions in the poleward edge of green-line aurora indicate that pulses of reconnection were also taking place locally. The background picture is consistent with that predicted for a radar immediately equatorward of the main cusp [*Davis and Lockwood*, 1996].

Enhanced ion-acoustic spectra are generally to be found inside or adjacent to regions of red auroral emission, indicating the presence of sharp conductivity gradients [*Collis et al.*, 1991; *Rietveld et al.*, 1991]. Current-driven instabilities are normally associated with soft electron precipitation, but from a study of narrow-angle images we have shown a correspondence between inferred field-aligned current bursts and energetic auroral precipitation. Our results indicate that within a single radar integration period, the beam can for part of the time be within a region of downward field-aligned current carried by upgoing thermal electrons. Within the same integration period the radar may be observing in regions of upward current carried by downward flows of thermalized electrons required by current continuity. In common with previous studies [e.g., *Collis et al.*, 1991; *Rietveld et al.*, 1991], we suggest that spectra with enhancements to both

ion-acoustic lines are due to either the radar sampling across different spatial structures or temporal variations within the integration period.

Acknowledgments. We thank the Director and Staff of the EISCAT Scientific Association for providing the radar data used in this work, and for their assistance in carrying out the experiment. EISCAT is an international facility supported by Finland, France, Germany, Japan, Norway, Sweden, and the United Kingdom. Thanks are due also the University of Calgary, the University of Alaska, Fairbanks, and Universitetsstudiene på Svalbard for data from various optical instruments. We benefited greatly from discussions with Antonius Otto of the University of Alaska, Fairbanks and Ian McCrea of the Rutherford Appleton Laboratory.

Michel Blanc thanks Jean-Pierre St.-Maurice and Francois Forme for their assistance in evaluating this paper.

References

Buchert, S. C., A. P. van Eyken, T. Ogawa, and S. Watanabe, Naturally enhanced ion-acoustic lines seen with the ESR, *Adv. Space Res.*, in press, 1999.

Cabrit, B., H. Opgenoorth, and W. Kofman, Comparison between EISCAT UHF and VHF backscattering cross section, *J. Geophys. Res., 101,* 2369–2376, 1996.

Collis, P. N., I. Häggström, K. Kaila, and M. T. Rietveld, EISCAT radar observations of enhanced incoherent scatter spectra: Their relation to red aurora and field-aligned currents, *Geophys. Res. Lett., 18,* 1031–1034, 1991.

Davis, C. J., and M. Lockwood, Predicted signatures of pulsed reconnection in ESR data, *Ann. Geophys., 14,* 1246–1256, 1996.

Elphic, R. C., M. Lockwood, S. W. H. Cowley, and P. E. Sandholt, Flux-transfer events at the magnetopause and in the ionosphere, *Geophys. Res. Lett., 17,* 2241–2244, 1990.

Farrugia, C. J., P. E. Sandholt, W. F. Denig, and R. B. Torbert, Observation of a correspondence between poleward moving auroral forms and stepped cusp ion precipitation, *J. Geophys. Res., 103,* 9309–9315, 1998.

Forme, F. R. E., A new interpretation on the origin of enhanced ion acoustic fluctuations in the upper ionosphere, *Geophys. Res. Lett., 20,* 2347–2350, 1993.

Forme, F. R. E., and D. Fontaine, Enhanced ion acoustic fluctuations and ion outflows, *Ann. Geophys., 17,* 182–189, 1999.

Forme, F. R. E., J.-E. Wahlund, H. J. Opgenoorth, M. A. L. Persson, and E. V. Evans, Effects of current driven instabilities on the ion and electron temperatures in the topside ionosphere, *J. Atmos. Terr. Phys., 55,* 647–666, 1993.

Forme, F. R. E., D. Fontaine, and J.-E. Wahlund, Two different types of enhanced ion acoustic fluctuations observed in the upper ionosphere, *J. Geophys. Res., 100,* 14,625–14,636, 1995.

Foster, J. C., C. del Pozo, K. Groves, and J.-P. St.-Maurice, Radar observations of the onset of current driven instabilities in the topside ionosphere, *Geophys. Res. Lett., 15,* 160–163, 1988.

Gosling, J. T., M. F. Thomsen, S. J. Bame, T. G. Onsager, and C. T. Russel, The electron edge of the low-latitude boundary layer during accelerated flow events, *Geophys. Res. Lett., 17,* 1833–1836, 1990.

Hapgood, M. A., and B. S. Lanchester, A narrow auroral arc observed with EISCAT, *J. Atmos. Terr. Phys., 49,* 49–55, 1987.

Karlson, K. A., M. Øieroset, J. Moen, and P. E. Sandholt, A statistical study of flux transfer event signatures in the dayside aurora: The IMF B_y-related prenoon-postnoon asymmetry, *J. Geophys. Res., 101,* 59–68, 1996.

Kindel, J. M., and C. F. Kennel, Topside current instabilities, *J. Geophys. Res., 76,* 3055–3078, 1971.

Lockwood, M., Solar wind–magnetosphere coupling, in *Incoherent Scatter: Theory, Practice and Science, Tech. Rep.* 97/53, EISCAT Sci. Ass., Ramfjordmoen, Tromsdalen, Norway, 1997.

Lockwood, M., W. F. Denig, A. D. Farmer, V. N. Davda, S. W. H. Cowley, and H. Luhr, Ionospheric signatures of pulsed reconnection at the Earth's magnetopause, *Nature, 361,* 424–428, 1993.

Rietveld, M. T., P. N. Collis, and J.-P. St.-Maurice, Naturally enhanced ion-acoustic waves in the auroral ionosphere observed with the EISCAT 933-MHz radar, *J. Geophys. Res., 96,* 19,291–19,305, 1991.

Rietveld, M. T., P. N. Collis, A. P. van Eyken, and U.-P. Løvhaug, Coherent echoes during EISCAT UHF Common Programs, *J. Atmos. Terr. Phys., 58,* 161–174, 1996.

Rosenbluth, M. N., and N. Rostoker, Scattering of electromagnetic waves by a non-equilibrium plasma, *Phys. Fluids, 5,* 776–788, 1962.

Sandholt, P. E., A. Egeland, and B. Lybekk, On the spatial relationship between auroral emissions and magnetic signatures of plasma convection in the midday polar cusp and cap ionospheres during negative and positive IMF B_z: A case study, *J. Geophys. Res., 91,* 2108–2112, 1986.

Stasiewicz, K., and T. Potemra, Multiscale current structures observed by Freja, *J. Geophys. Res., 103,* 4315–4325, 1998.

Stasiewicz, K., G. Holmgren, and L. Zanetti, Density depletions and current singularities observed by Freja, *J. Geophys. Res., 103,* 4251–4260, 1998.

St.-Maurice, J.-P., W. Kofman, and D. James, In situ generation of intense parallel electric fields in the lower ionosphere, *J. Geophys. Res., 101,* 335–356, 1996.

Trondsen, T. S., and L. L. Cogger, High-resolution television observations of black aurora, *J. Geophys. Res., 102,* 363–378, 1997.

Velichko, V. A., N. E. Molochuskin, V. P. Samsonov, and S. R. Smotritskiy, The orientation of rays with a short lifetime in the active corona of polar aurora, *Geomagn. Aeron., 25,* 729–731, 1985.

Wahlund, J.-E., F. R. E. Forme, H. J. Opgenoorth, and M. A. L. Persson, Scattering of electromagnetic waves from a plasma: Enhanced ion acoustic fluctuations due to ion-ion two-stream instabilities, *Geophys. Res. Lett., 19,* 1919–1922, 1992a.

Wahlund, J.-E., H. J. Opgenoorth, I. Häggström, K. J. Winser, and G. O. L. Jones, EISCAT observations of topside ionospheric ion outflows during auroral activity: Revisited, *J. Geophys. Res., 97,* 3019–3037, 1992b.

Wahlund, J.-E., H. J. Opgenoorth, F. R. E. Forme, M. A. L. Persson, I. Häggström, and J. Lilensten, Electron energization in the topside auroral ionosphere: On the importance of ion-acoustic turbulence, *J. Atmos. Terr. Phys., 55,* 623–645, 1993.

Wannberg, G., et al., The EISCAT Svalbard Radar: A case study in modern incoherent scatter radar system design, *Radio Sci., 32,* 2283–2307, 1997.

B. S. Lanchester, and M. H. Rees, and K. J. F Sedgemore-Schulthess, Department of Physics and Astronomy, University of Southampton, Highfield, Southampton, Hampshire SO17 1BJ, England. (e-mail: bsl@phys.soton.ac.uk; mhr@phys.soton.ac.uk; kjfs@phys.soton.ac.uk)

M. Lockwood, Space Science Department, Rutherford Appleton Laboratory, Chilton, Didcot, Oxon OX11 0QX, England. (e-mail: m.lockwood@rl.ac.uk)

D. A. Lorentzen and J. Moen, Universitetsstudiene på Svalbard, Postboks 156, N-9170 Longyearbyen, Norway. (e-mail: dagl@unis.no; jmoen@unis.no)

T. S. Trondsen, Institute for Space Research, Department of Physics and Astronomy, University of Calgary, 2500 University Drive NW, Calgary, Alberta, Canada TN2 1N4. (e-mail: trondsen@phys.ucalgary.ca)

(Received November 2, 1998; revised June 4, 1999; accepted June 16, 1999.)

associated with auroral arcs, high electron temperatures, and weak to moderate perpendicular electric fields. *Wahlund et al.* [1993] suggest that the electron heating events observed along with enhanced spectra are the result of ion-acoustic turbulence in addition to collisional heating by precipitating beam electrons. They propose also that ion-acoustic turbulence may account for the soft electron precipitation and field-aligned ion outflows observed during these events. *Forme et al.* [1993] use a theoretical model to investigate the heating effects of low-frequency plasma turbulence caused by current-driven instabilities in the topside ionosphere.

Forme et al. [1995] present mainland EISCAT observations displaying two distinct types of spectral enhancement. One type relates to high electron temperatures, strong ion outflows, an altitude extent of 300–700 km, and auroral arcs; the other corresponds to slightly enhanced electron temperatures, no ion outflows, a lower altitude extent (100–200 km), and an apparent lack of low-energy precipitating particles. *Cabrit et al.* [1996] present results showing significant differences between measurements made with the EISCAT UHF and VHF radar systems and discuss these in terms of wavenumber dependence, inhomogeneous scattering cross sections, and small-scale auroral arcs, suggesting that coherent echoes may be located preferentially beside subkilometer scale features. Finally, *Rietveld et al.* [1996] present results of a statistical survey of over 5000 hours of mainland EISCAT data, finding, on average, coherent echoes in around 170 data dumps per million, an increased occurrence of such echoes during sunspot maximum, no seasonal dependence, and a weak minimum in the morning sector.

In this paper we present examples of enhanced spectra recorded by the EISCAT Svalbard Radar (ESR) observing along the local magnetic field direction in the vicinity of the dayside cusp/cleft, along with simultaneous optical measurements made with a meridian scanning photometer and a narrow-angle TV imager. The first examples of enhanced spectra seen with the ESR have been reported recently by *Buchert et al.* [1999]. We discuss the various theories put forward to explain enhanced radar spectra and, assuming a current-driven instability model, investigate the relationship between coherent spectra and field-aligned currents, relating the inferred currents to the auroral emissions seen, including optical signatures of time-varying magnetic reconnection.

2. Experiment

The EISCAT Svalbard Radar is situated near Longyearbyen on the arctic archipelago of Svalbard. The 500-MHz ESR system [see *Wannberg et al.*, 1997] began operations in March 1996 and is now used routinely in both common and special program mode. The data presented here were taken in January 1998 and comprise measurements using the "GUP0" experiment with the beam pointed along the local magnetic field direction at an elevation of 81.5°. The modulation scheme for GUP0 has four long pulses transmitted in sequence: three of 360-μ s duration and one of 150 μs. ESR raw data are stored as lag profiles rather than as gated autocorrelation functions. Standard practice is to allow the gating to vary with range according to the scale height of the atmosphere, but the highest range resolution obtainable is restricted by the zero-lag resolution (58.5 km in the case of GUP0) and the range ambiguity function. The 10-s raw data dumps are analyzed in order to give ionospheric parameters such as electron density, electron and ion temperatures, and line-of-sight ion velocity.

A Meridian Scanning Photometer (MSP), owned by the University of Alaska, Fairbanks and situated in Adventdalen near the ESR, was operational throughout the campaign. The Adventdalen MSP is a four-channel instrument with tilting filters mounted on the photomultipliers in order to record peak and background emissions. By tilting the filters, the transmission wavelength is shifted by 1.2–1.5 nm from the base wavelength. Light is collected by a mirror which rotates about an axis perpendicular to the magnetic meridian plane, and each channel has a roughly 2° circular field of view. We make use of three channels: 630.0, 427.8 and 557.7 nm. The instrument scans through 180 positions along the meridian from the northern to southern horizons with a cycle time of 16 s, recording peak and background emissions twice in each position. A measurement is obtained by subtracting the average of the two background readings from the average of the two peak readings in each position.

The University of Calgary Portable Auroral Imager (PAI) is a narrow-angle TV imager designed for high-resolution optical measurements of auroral phenomena [*Trondsen and Cogger,* 1997]. The camera achieves very high sensitivity through the use of an 18-mm GEN III image intensifier with a quantum efficiency of around 30% throughout the 600 to 900-nm wavelength range. During the campaign the camera was pointed toward the magnetic zenith and a 50-mm objective lens was used, giving a linear coverage at 105 km altitude of around 30 × 20 km and a resolution better than 100 m. Onto this lens was fixed a 675-nm cutoff filter, used in order to suppress the slower emissions and focus instead on the N_2(1PG) and N_2^+(Meinel) bands. The filter significantly reduces the amount of light available to produce an image, but the exceptionally short lifetimes of these excited electronic states allow fast moving, more discrete auroral forms to be resolved.

3. Observations

In this paper we concentrate on a 3-hour period from the morning of January 24, 1998, during a coordinated radar and optical campaign on Svalbard. In an attempt to study fast changes in the aurora by comparison with video images from the PAI, the radar data are analyzed with a 10 s resolution, and in order to extract the maximum amount of information from the signal all four pulses are merged in the analysis. This leads to a slight but systematic underestimation of electron density in the first few points from each pulse, but as we are not interested here in absolute values of electron density this is not a problem. The electron and ion temperatures, together with the line-of-sight ion velocities, are unaffected by pulse merging. At the time the experiment was carried out, ground clutter so severely affected the alternating codes

used for E region measurements that we use only long-pulse data from altitudes of 155 km and above.

Plate 1 gives an overview of the ESR observations for 0500–0800 UT (around 0815–1115 MLT), January 24, 1998. From top to bottom the panels display electron density N_e, electron temperature T_e, ion temperature T_i, and line-of-sight ion velocity V_i (positive upward), all color-coded as a function of altitude and observation time. There are three initial N_e and T_e enhancements seen in the ESR data at 0526, 0531, and 0536 UT. Subsequently, there are a series of density enhancements very similar to those predicted by *Davis and Lockwood* [1996] for the equatorward cusp edge in the presence of pulsed reconnection.

Plate 2 shows column emission rates observed with the MSP as a function of zenith angle and time for wavelengths of 630.0 nm (red), 427.8 nm (blue), and 557.7 nm (green). From 0535 UT, the green-line emissions illustrate the effect of a major pumping up of the ring current by injection of energized particles, and this enhanced emission toward the south helps to mark the border between open and closed field lines. Poleward of the radar beam (elevation angle 81.5°), there is a 630-nm dominant region associated with magnetosheath particles entering the cusp on open field lines, and around the magnetic zenith there are some green and blue emissions which we believe to be associated with bursts of strong field-aligned currents. The red-line data show a series of poleward moving enhancements characteristic of southward interplanetary magnetic field (IMF) [*Sandholt et al.*, 1986]. This is supported by all-sky camera images that show the events moving poleward and to the west, consistent with the prevailing IMF $B_y > 0$ observed by the Wind satellite.

Strong ion upflows can be seen in Plate 1 starting at around 0545 UT. Height profiles of line-of-sight ion velocity indicate a transition at an altitude of around 250 km, above which the velocity increases rapidly to values of 500 m s^{-1} and greater at 500 km altitude. These outflows are sustained until 0730 UT and are broadly associated with the precipitation events seen in the electron density and temperature measurements at lower altitudes.

The analysis of incoherent scatter radar involves the fitting of theoretical spectra to raw data. There are a number of assumptions built into this, the principal one as far as our work is concerned being that of a near-Maxwellian plasma. Departures from thermal equilibrium can lead to a failure of the fitting procedure in the most extreme cases and may have more subtle effects in less extreme cases. One way in which to test the goodness of fit in is to specify a maximum number of iterations in the analysis. A better method with which to search through large volumes of data for gross spectral asymmetries has been described by *Rietveld et al.* [1996]. If the spectra are in any way typical of thermal plasma and the signal-to-noise ratio is reasonably high, most should fit within five iterations. Spectra that do not fit within a few iterations are almost certainly unusual in form and the analysis of such could lead to spuriously large derived electron densities and electron and ion temperatures. Our procedure identifies both dramatically enhanced spectra, such as are found by the *Rietveld et al.* [1996] method, and more subtly distorted spectra. Likely candidates for enhanced spectra are identified in the analysis by flagging those dumps which exceed the maximum iterations maximum criterion over a considerable altitude range. In this way we found a total of five events in which enhanced spectra were present. Two of these events are presented.

Figure 1 displays ESR ion spectra from four consecutive 10-s dumps, starting at 0700:30 UT. In Figures 1a–1d the time given is the end of the integration period. Each figure shows the range-corrected power spectral density, both as grey scale maps and as stacked line plots (smoothed in the frequency domain with cubic splines), plotted in each case as a function of range and Doppler shift. Those in Figure 1a (0700:30 UT) are typical of incoherent scatter from thermal plasma, with two "humps" placed symmetrically around the zero frequency line and the offset of the peaks increasing with altitude owing to an increase in ion temperature. The magnitude of the peaks decreases with altitude owing to a decrease in plasma density in the topside ionosphere. By 0700:40 UT (Figure 1b) both lines are enhanced at higher altitudes, with the degree of enhancement increasing with height up to around 1 order of magnitude in total backscattered power. The upshifted ion line is enhanced slightly above that of the downshifted line at lower altitudes, with the situation reversed above 350 km. Enhanced upshifted ion lines (i.e., positive frequency offset) correspond to downward propagating ion-acoustic waves, or downward streaming thermal electrons. In the following dump (Figure 1c), the downshifted ion line is so enhanced that all other echoes are suppressed by the required dynamic range of the plot scale. By 0701:00 UT (Figure 1d) the situation has returned to normal, with typical incoherent scatter spectra.

In order to study the ionospheric conditions at the times when enhanced spectra were seen, we carried out a detailed analysis of the 0700:30 and 0701:00 UT data dumps. These times were chosen since they are the closest to those of the enhanced spectra. Fitting plasma parameters to enhanced ion spectra would invalidate the assumption of thermal equilibrium, although *Forme and Fontaine* [1999] show that it may be possible to extract some estimates of electron temperature and ion velocity within turbulent regions. Figure 2 shows the electron and ion temperatures and ion velocities for both times as a function of altitude. Taking into account the random errors, at neither time is the ion temperature particularly large, indicating that any perpendicular electric field present is either small in magnitude or short-lived. The topside electron-to-ion temperature ratio is around 3, which is typical for these kinds of events [e.g., *Collis et al.*, 1991; *Rietveld et al.*, 1991; *Wahlund et al.*, 1993], and the ion velocity shows an increase with height up to around 200 m s^{-1} at 500 km altitude. Note that this is far lower than the peak values measured between 0600 and 0800 UT.

PAI images for the 20 s covering the time of the enhanced radar spectra are displayed in Figure 3. There is one panel per second in time, each with four video frames averaged in order to improve the signal-to-noise ratio by a factor of 2. In the images, north is at the top and east is to the right. The field of view is 16° × 12°, with the south-north ele-

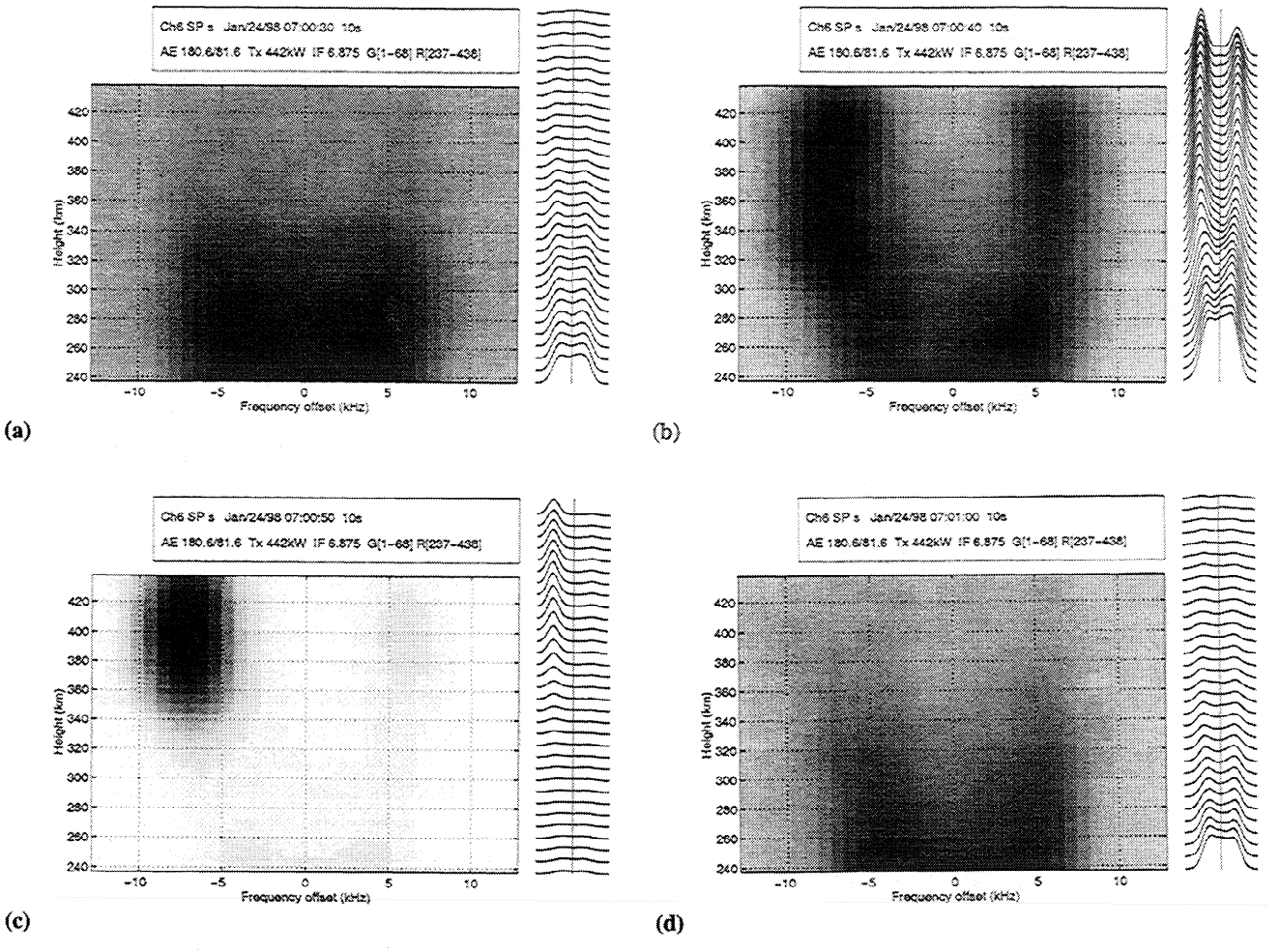

Figure 1. EISCAT Svalbard Radar long-pulse spectra from four consecutive 10-s dumps: 0700:30–0701:00 UT, January 24, 1998. Figures 1a and 1d show spectra typical of incoherent backscatter, while Figures 1b and 1c show varying degrees of ion-line enhancement.

vation range being 75.5°–87.5°. Owing to the use of the 675-nm cutoff filter, the intensities recorded are somewhat low, and so an enhanced scale is used in the image processing to improve the contrast. What Figure 3 serves to show is that within a single 10-s radar integration much can change within the radar sampling volume. Specifically, within the 0700:30 to 0700:50 UT period when enhanced spectra are seen, luminosity is sometimes present and sometimes absent in the radar beam (marked by a circle in the top left panel). This may have serious consequences for the analysis of radar data, and it is an important point to which we will return. Common to all the examples of enhanced radar spectra that we have found is the existence in narrow-angle images of bright coronal forms and small patches of luminosity in the magnetic zenith. A survey of all the images for the 3-hour period shows that coronal forms were not observed at any time other than when enhanced radar spectra were seen. The presence of a coronal form indicates that, taking into account the height of the emission, one is observing a region directly adjacent to the field line down which auroral precipitation is occurring. Looking directly up that field line, one would see a bright patch of luminosity. In some cases coronal forms coexist with luminosity within the area covered by the radar beam; in other cases they do not.

For the second example, Figure 4 shows four consecutive ESR spectra from 0706:20 UT. Figure 4a shows an ion spectrum typical of incoherent scatter from thermal plasma. In the following dump (0706:30 UT) the downshifted ion line is enhanced over a restricted range between 340 and 440 km altitude. This may look like satellite contamination, but the Doppler shift indicates that the enhancement is geophysical in origin. At 0706:40 UT the upshifted line is enhanced from the lowest altitudes sampled up to around 430 km, above which there is a switch to a downshifted ion line. By 0706:50 UT, only the downshifted line is enhanced, particularly at higher altitudes.

Repeating the analysis of thermal spectra measured by the ESR, we see in Figure 5 a similar situation in which the ion temperature is not significantly enhanced by Joule heating due to a perpendicular electric field, a relatively high electron temperature, and a line-of-sight ion velocity increasing sharply above 300-km altitude. Again, the magnitude of the